Palaeogeography, Palaeoclimatology, Palaeoecology 496 (2018) 155–165

Contents lists available at ScienceDirect

Palaeogeography, Palaeoclimatology, Palaeoecology

journal homepage: www.elsevier.com/locate/palaeo

The respective characteristics of millennial-scale changes of the India summer monsoon in the Holocene and the Last Glacial

Bing Hong[a], Masao Uchida[b], Yetang Hong[a,*], Haijun Peng[a], Miyuki Kondo[b], Hanwei Ding[a]

[a] State Key Laboratory of Environmental Geochemistry, Institute of Geochemistry, Chinese Academy of Sciences, 99 Lincheng Road West, Guiyang, Guizhou 550081, China
[b] Center for Environmental Measurement and Analysis, National Institute for Environmental Studies, Onogawa 16-2, Tsukuba, Ibaraki 305-0053, Japan

ARTICLE INFO

Keywords:
Extreme climate event
Abrupt climate change
Global warming
Bond event
Peat

ABSTRACT

There has been no proxy climate record simultaneously showing the identified millennial-scale change events of the India summer monsoon (ISM) during the period from the Last Glacial period to the Holocene, although these abrupt changes have been shown in separate records. This deficiency prevents further understanding of the potentially different characteristics of the ISM rapid changes. Here, we present a 33,300-year record of the ISM reconstructed from the stable carbon isotopic composition of cellulose in peat deposits collected near the Tibetan Plateau, reflecting the millennial-scale history of abrupt changes in the ISM intensity from the cold late Last Glacial to the warm Holocene epoch. Our record shows that, corresponding to the abrupt cooling (warming) events that occur in the high northern latitudes, the ISM intensity abruptly decreases (increases), which provides additional evidence for the teleconnection between low-latitude monsoonal variability and the rapid temperature fluctuation of high northern latitudes. However, this relationship behaves differently in the cold and warm stages. In the cold late Last Glacial period, a one-to-one response is often seen, but in the warm Holocene, the ISM often shows only partial responses to the rapid cooling events. In particular, more than half of the abruptly weakening events in the ISM occur in the Holocene, and the amplitudes of declines are larger in the warm stage than in the cold stage, which reveals that extreme change events in the ISM have occurred much more in the warm Holocene and may have once influenced the development of ancient civilizations. We consider that the various characteristics of the abrupt changes in the ISM during the warm and cold stages may have derived from different combinations of climatic drivers within the two stages. These results provide a historical record of the considerable changes in ISM and resultant effects on human society, and so provide a background for concerns over contemporary climate change.

1. Introduction

Abrupt millennial climate change reflects a rapid step-like shift phenomenon in climate variability that has occurred repeatedly in Earth history and differs from the slow climate variation caused by the change of the relative position between the Earth and the Sun (Overpeck and Webb, 2000). A series of abrupt temperature changes has been perfectly recorded in the Greenland GISP2 ice core (Johnsen et al., 1992; Dansgaard et al., 1993; Stuiver and Grootes, 2000) and ice-rafted debris (IRD) sediments of the North Atlantic (Bond et al., 2001). Correspondingly, abrupt changes in the intensity of the India summer monsoon (ISM) during the Holocene Epoch (Gupta et al., 2003; Fleitmann et al., 2003; Hong et al., 2003; Wang et al., 2005; Dykoski et al., 2005) and the last deglaciation (Yuan et al., 2004) have also been observed. Comparing the ISM records with both the climate processes from the high northern latitudes and the other physical processes associated with global changes has resulted in the presentation of several hypotheses concerning the mechanism of abrupt change of the ISM in the Holocene (Gupta et al., 2003; Fleitmann et al., 2003; Hong et al., 2003; Yuan et al., 2004; Wang et al., 2005; Wanner et al., 2011). The study of the millennial change in the ISM can be traced back to a more distant past. In 1998, a group of high-resolution records from the West Arabian Sea for the first time reported a series of abrupt millennial-scale changes of the ISM intensity in the glacial period and their teleconnection with variations of the high northern latitude climate (Schulz et al., 1998). Later, several monsoon records from the Bay of Bengal and the West Arabian Sea reproduced the abrupt weakening of the ISM in response to the suddenly cooling climate at the high northern latitudes (Kudrass et al., 2001; Ivanochko et al., 2005; Deplazes et al., 2014). However, there has been no ISM record within the continental area that has reproduced the above phenomenon revealed by Schulz et al., although the splicing of $\delta^{18}O$ records from five stalagmites in

* Corresponding author.
E-mail address: hongyetang@vip.skleg.cn (Y. Hong).

https://doi.org/10.1016/j.palaeo.2018.01.033
Received 11 October 2017; Received in revised form 21 January 2018; Accepted 22 January 2018
Available online 01 February 2018
0031-0182/ © 2018 Elsevier B.V. All rights reserved.

Hulu Cave has clearly shown abrupt changes of the East Asian summer monsoon (EASM) and their teleconnection with the high northern latitude climate variations during the Pleistocene (Wang et al., 2001). In particular, there has also been no long ISM record to date that has simultaneously shown all of the identified millennial-scale changes of the ISM during the period from the Glacial to the Holocene. These deficiencies prevent further revelation of the possible similarities and differences of the ISM abrupt changes in the cold Glacial and the warm Holocene and encourage paleoclimatologists to develop more sensitive and longer proxy records to better understand the abrupt change characteristics and mechanisms of the monsoon. Here, we present a 33,300-year time series of the ISM intensity reconstructed from the stable carbon isotopic composition ($\delta^{13}C$) of cellulose in peat deposits collected near the Tibetan Plateau, which provides us with an opportunity to examine further the characteristics of the ISM abrupt millennial changes and their dynamic mechanisms during the interval from the late Last Glacial to the Holocene.

2. Study region and methods

The sampling site for this study is a valley peat bog at an altitude of 1950 m above sea level. It is located in Baoan Village, Yuexi County of Sichuan Province, southwestern China, which is in the Hengduan Mountains at the southeastern edge of the Tibetan Plateau (Fig. 1). The Hengduan Mountains comprise a series of approximately parallel southwest-northeast mountain ranges originating from the compression of the Indian Plate into the Eurasian Plate. The height of the northern mountains is between 4500 and 5000 m above sea level, and this height gradually decreases toward the south, dropping to less than 3000 m in the Yunnan region. In general, the difference in altitude between the ridges and valleys is approximately 2000 m. With high ridges and deep valleys, the mountains block east-west travel, hence their name 'Hengduan', which means 'cut across' in Chinese. However, because of their southwest-northeast orientation, the mountains have become a delivery channel for the transmission of water vapor from the ISM. An investigation of the moisture sources of June–July-August precipitation in the Heqing district (Site 4 in Fig. 1) southwest of Baoan shows that more than 90% of the moisture for summer precipitation originates from the ISM (An et al., 2011; Kalnay et al., 1996), which supports the previous conclusion that approximately 90% of the moisture flux into southern Asia and its adjacent areas is caused by the cross-equatorial ISM (Clemens et al., 1996). The geographical characteristics of the Baoan distract located in lower latitudes and higher altitudes created a northern subtropical monsoon climate. The climate in the summer and autumn are moist and cool, and the winter and spring are dry and cold. The annual average temperature in the Baoan district is approximately 13 °C, and the annual mean rainfall is approximately 1000 mm. Annual effective accumulated temperature greater than or equal to 10 °C is approximately 4000 °C. Yunnan pine (*Pinus yunnanensis*) and evergreen sclerophyllous oaks (*Quercus senescens*, *Quercus rehderiana*, and *Quercus gilliana*) dominate the vegetation around the Baoan peatland. The humid and cool climate of this mountain region has promoted the development of a thick peat sediment layer. Therefore, the peatland in the Hengduan Mountains in southwestern China is ideally positioned to capture ISM signals (Fig. 1).

In the past more than a century the peat-based paleoclimate research has developed a wide range of proxy-climate indicators (Table 1 of Chambers et al., 2012). Many expositions about the principle of the $\delta^{13}C$ value of C3 vascular plants in peat as a proxy indicator for monsoon rainfall have been also held during the last two decades (Hong et al., 2001, 2003, 2010, 2014a, 2014b; Ménot and Burns, 2001; Amesbury et al., 2015). They all stress that, based on studies of the photosynthesis process of C3 vascular plants, plant physiologists have proposed a formula to describe how plant leaf stomatal conductance exerts a controlling effect on the $\delta^{13}C$ value of the plant (Francey and Farquhar, 1982; Farquhar et al., 1989; Schleser, 1995). Environmental factors such as temperature, light, and CO_2 concentration, etc. have little influence on the $\delta^{13}C$ value of C3 vascular plants. The environmental relative humidity, however, is the most important factor. When the relative humidity is low, a large leaf to air vapor pressure deficit occurs between the saturated sub-stomatal cavity and the relatively dry atmosphere. The plant leaf stomata shrink to reduce the rate of passive water loss under such dry conditions. However, this physiological process of plants also reduces the rate of inward CO_2 diffusion and creates a pool of CO_2 inside the leaf that experiences reduced interaction with atmospheric CO_2. As plants continue to assimilate carbon and prioritize the use of ^{12}C, the ^{13}C content in the pool becomes gradually enriched, which eventually leads to the emergence of higher $\delta^{13}C$ values. Conversely, increases in the environmental relative humidity cause stomatal opening, which is conducive to the diffusion of CO_2 into the plant and ultimately leads to lower $\delta^{13}C$ values (Hong et al., 2001; Ménot and Burns, 2001; Amesbury et al., 2015). It is worth emphasizing that the water availability should have a smaller effect on vascular plants than on non-vascular plants because of the ability of C3 vascular

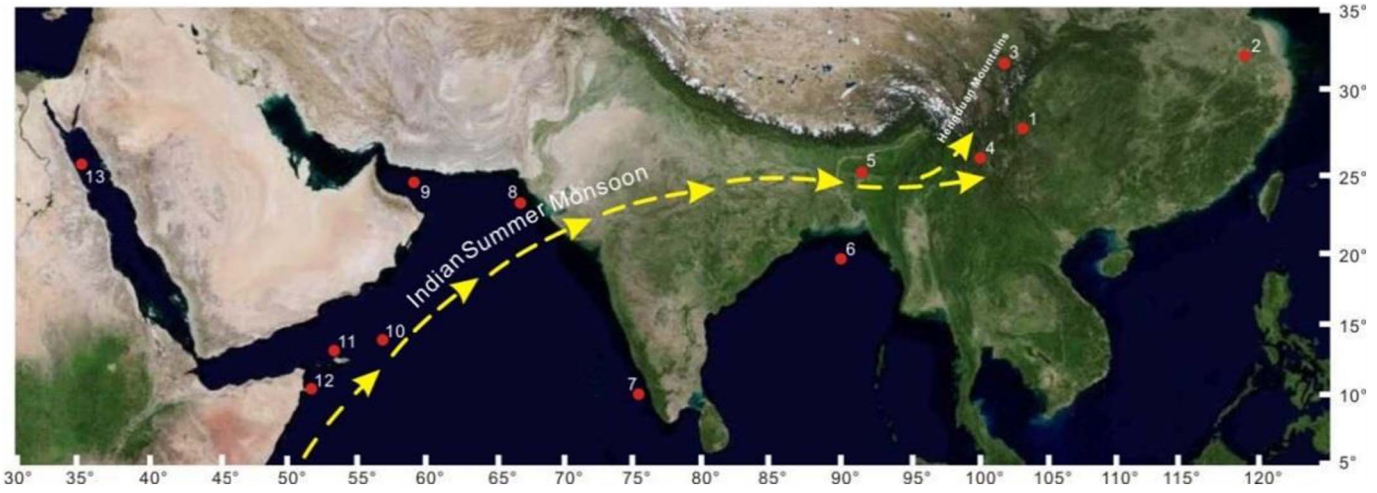

Fig. 1. Map showing the sampling site for this study, the relative research sites, and sketches of the Indian summer monsoon. Site 1–Baoan (this study). Site 2–Hulu (Wang et al., 2001). Site 3–Hongyuan (Hong et al., 2003). Site 4–Heqing (An et al., 2011). Site 5–Mawmluh (Berkelhammer et al., 2012). Site 6–KL 126 core (Kudrass et al., 2001). Site 7–GC-5 core (Thamban et al., 2001). Site 8–136 KL core (Schulz et al., 1998). Site 9–M5-422 core (Cullen et al., 2000). Site 10–74KL core (Sirocko et al., 1993). Site 11–4018G core (Tiwari et al., 2010). Site 12–Core 905 (Ivanochko et al., 2005). Site 13–GeoB 5836-2 core (Arz et al., 2006). The base map of Fig. 1 was obtained from GoogleMaps using screenshot software and then additions to the map were made using CorelDRAW Graphics Suite 12.

plants to regulate water uptake and loss via stomatal conductance and to develop deep and/or extensive root systems. Alternatively, the effects of environmental relative humidity on stomatal conductance and stomatal control of CO_2 assimilation and the effects of these processes on photosynthesis and water use efficiency are the main controlling factors of carbon isotope fractionation in vascular plants. Therefore, the $\delta^{13}C$ signal in C3 vascular plants is influenced by differences in the prevailing climate to a greater extent compared with the site-specific differences in surface moisture (Amesbury et al., 2015), which explains why measurements at different spatial scales consistently indicate that there is a negative correlation between the $\delta^{13}C$ values of C3 vascular plants or organic matter and the levels of rainfall or humidity (Lee et al., 2005; Wang et al., 2008; Diefendorf et al., 2010; Ren and Yu, 2011). In summary, the $\delta^{13}C$ values of C3 vascular plants, which are preserved in plant organic matter, may provide a sensitive record of changes in rainfall, especially during the period of plant growth. Plant cellulose is one of the most stable components in plant organic matter. Both cellulose and its isotopes are highly stable over periods of approximately 10^5 years (Briggs et al., 2000). Therefore, the $\delta^{13}C$ of C3 vascular plant cellulose has been used as a sensitive bioindicator for the monsoon rainfall variation. Lower $\delta^{13}C$ values in the peat cellulose indicate larger amounts of summer rainfall or a stronger ISM intensity, and higher $\delta^{13}C$ values indicate smaller amounts of summer rainfall or a weaker ISM (Hong et al., 2001, 2003).

An approximately 10.1-m-long peat core (28°47′N, 102°57′E) was extracted from the Baoan peatland using a Russian peat corer. Based on identification of the morphology of the macrofossils in peat by microscopic analysis, it is estimated that approximately 80% of the plant residues in the Baoan peat core sample belong to vascular sedge family of C3 plants, including *Carex* and *Kobresia*. *Sphagnum* occurs in small amounts. The peat core sample was cut contiguously into 1 cm subsamples corresponding to a mean time resolution of approximately 33 years. We used a sodium chlorite oxidation method to extract alpha cellulose from the peat vegetation residues (Green, 1963; Hong et al., 2001, 2003). Approximately 20 mg of cellulose sample could be extracted from every 1.5 g of dry peat sample. These cellulose samples were used for measurements of the $\delta^{13}C$ and ^{14}C values. To determine the $\delta^{13}C$ of the peat cellulose, approximately 2 mg of the cellulose samples was loaded into a borosilicate tube together with preheated copper (II) oxide. After drying under vacuum conditions, the tube was sealed with an oxy-gas torch and heated in a muffle furnace at 550 °C (Hong et al., 2001, 2003; Sofer, 1980). The resulting CO_2 gas was measured for stable isotopes using a MAT-252 mass spectrometer. The stable carbon isotopic composition of cellulose is expressed as $\delta^{13}C = \left[\frac{(^{13}C/^{12}C)_{sample}}{(^{13}C/^{12}C)_{standard}} - 1\right] 1000‰$ (Coplen, 2011). All results are reported in parts per mil (‰) relative to VPDB, and the precision is better than ± 0.1‰ (1σ) based on the replicate analyses of laboratory standards with the $\delta^{13}C_{IAEA\text{-}C3}$ value of −24.91‰. To build the ^{14}C age timescale, we first described the properties of the peat column samples collected on the field sampling spot and subdivided the column samples into several small fractions according to the color and texture changes of the fresh peat samples. The color and texture of each small fraction were the same; thus, correspondingly, the sedimentary environment and rate of accumulation of each small fraction were considered to be consistent. Radiocarbon samples were used to bracket the changes in the core sediment, and additional ages were then used to further secure the chronology. Finally, 29 ^{14}C age control points were selected (Fig. 2 and Table 1). The peat cellulose samples from the control points were prepared for graphite targets, and their ^{14}C intensities were determined at the AMS Laboratory of the National Institute for Environmental Studies in Tsukuba, Japan, to determine the ^{14}C ages of the samples (Uchida et al., 2008). The chronological age was obtained after performing a correction using the CALIB 6.1 program (Reimer et al., 2009). We then obtained a calibrated ^{14}C age sequence for the Baoan peat profile via linear interpolation and a $\delta^{13}C$ time series spanning 33,300 years, of which a $\delta^{13}C$ time series corresponding approximately to the upper 6-m portion of the core sample (representing dates from 17.5 to approximately 0 cal kyr BP) has previously been published to document the phase relationship between the ISM and the EASM during the last deglaciation (Hong et al., 2014b). For the natural output, the mean sedimentation rate of the entire Baoan peat profile was approximately 30.3 cm per 1000 years, which was sufficient to resolve millennial-scale variability.

3. Results and discussion

3.1. Variation of the ISM intensity on Milankovitch timescales

Fig. 3G shows that the ISM intensity inferred from Baoan peat cellulose $\delta^{13}C$ was generally weaker during the period from approximately 33 to 17 cal kyr BP. After experiencing oscillation during the last deglaciation, the ISM entered a stronger stage in the Holocene Epoch. This variation pattern shown by the Baoan peat record from the Tibetan plateau region is generally consistent with previously reported phenomena; that is, on the glacial-interglacial timescale, the ISM has been in general weaker during the cold Glacial and stronger during the warm Holocene, which has been documented by various types of proxy climate records from the Arabian Sea and Bay of Bengal (Fig. 3A–F) (Sirocko et al., 1993; Schulz et al., 1998; Kudrass et al., 2001; Thamban et al., 2001; Ivanochko et al., 2005; Tiwari et al., 2010).

The driving mechanism for the ISM on Milankovitch timescales has always attracted great attention from paleoclimatologists. In the early 1980s, Kutzbach proposed that the ISM intensity variations are primarily driven by northern summer insolation at the precession period (Kutzbach, 1981). The timing of the ISM strength has a small phase lag relative to maxima of the northern precession-driven radiation (Rossignol-Strick, 1983; Kutzbach and Street-Perrott, 1985; Ruddiman, 2006). These results have contributed to the development of climate model studies. Over time, however, a different hypothesis related to multiple forcing mechanisms has emerged. Clemens and Prell (1990, 2003) demonstrate that there is a significant lag between northern summer insolation maxima and the monsoon response. They suggest that the ISM system has been externally forced by cyclical changes in solar radiation and internally phase-locked to the transport of latent heat from the southern subtropical Indian Ocean to the Tibetan Plateau. In contrast to the results of the general circulation model, the climate change associated with variability in global ice volume is not a primary factor in determining the strength and timing of the monsoon (Clemens et al., 1991; Clemens and Prell, 2007). An et al. (2011) further reveal the importance of both Northern and Southern Hemisphere processes in driving monsoon variability. They suggest that at the glacial-interglacial timescales, interglacial ISM reaches a maximum, and the glacial ISM reaches a minimum, which reflect the impacts of the Indian low variation associated with global ice volume change. In particular, the proxy record of the ISM inferred from Heqing in Yunnan Province, southwestern China (Site 4 in Fig. 1) shows that the glacial ISM actually begins to increase before global ice volume reaches a maximum (Fig. 3 of An et al., 2011). This early strengthening has been attributed to an increased cross-equatorial pressure gradient derived from Southern Hemisphere high-latitude cooling (An et al., 2011). The results noted above show that, at Milankovitch timescales, the influence of internal feedback mechanisms in the Earth system on the ISM is much greater than previously thought, which is an issue worthy of in-depth study.

3.2. Characteristics of millennial-scale variation of ISM intensity

The Baoan peat cellulose $\delta^{13}C$ record shows a series of millennial-scale variations superimposed on the long-term trend of the ISM intensity variation (Fig. 4). These abrupt variations show different characteristics for the cold and warm stages during the past 33,300 years.

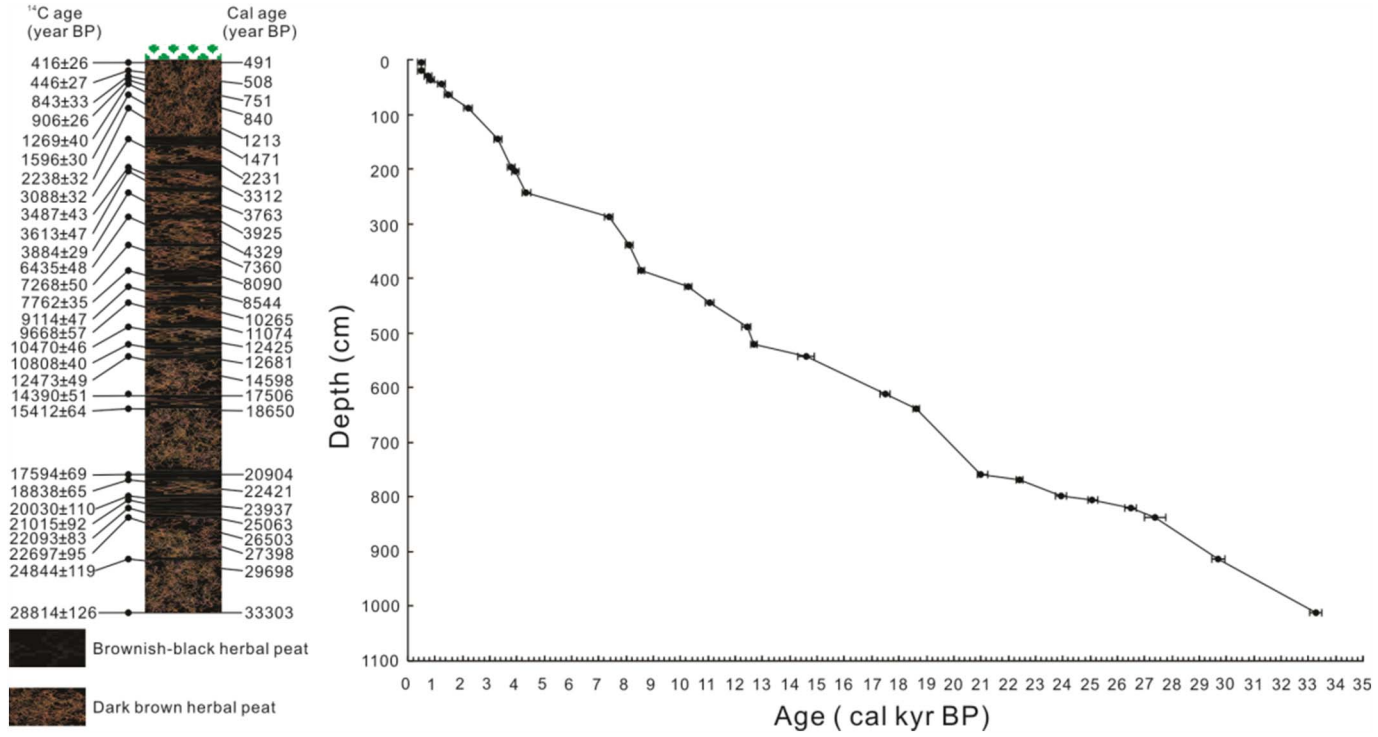

Fig. 2. Chronology and lithology of the fresh peat core from the Baoan peat bog. Black error bars show the cellulose ^{14}C dates with a 1σ error for the Baoan peat profile.

3.2.1. Millennial-scale variability of ISM intensity during the late Last Glacial and the last deglaciation

Fig. 4 shows that, corresponding to the several cooling events in the high northern latitude region inferred from the light (^{18}O-depleted) $\delta^{18}O$ values in the Greenland GISP2 ice core, including the Younger Dryas (YD) and the Heinrich events 1–3 (H1 − H3) (Fig. 4A), the contents of total organic carbon (TOC) in sediment cores taken from oxygen-minimum zone (OMZ) water depths along the continental margin off Pakistan in the northeastern Arabian Sea clearly decrease (Fig. 4B). In contrast, corresponding to the warming events inferred from the heavy $\delta^{18}O$ values in the GISP2 ice core, including the Bølling-Allerød (B/A) event and the Dansgaard-Oeschger (D/O) events or oscillations 2–5, the TOC contents from the OMZ increase (Schulz et al., 1998). The variations of the TOC content from the OMZ have been

Table 1
Radiocarbon dates of Baoan peat profile, Yuexi County.

Lab code	Sample ID	Depth (cm)	$\delta^{13}C$ (‰, VPDB)	^{14}C age (yr BP)	Calibrated age range (yr BP)	Calibrated age (yr BP)
TERRA-120310a25	YXI01	1	−24.53	416 ± 26	477–509	491
TERRA-120310a16	YXI02	14	−24.95	446 ± 27	497–518	508
TERRA-121610a12	YXI03	24	−24.38	843 ± 33	700–787	751
TERRA-120310a23	YXI04	33	−25.24	906 ± 26	782–904	840
TERRA-113010b14	YXI05	40	−26.40	1269 ± 40	1176–1267	1213
TERRA-120310a14	YXI06	59	−26.18	1596 ± 30	1417–1528	1471
TERRA-120310a26	YXI07	84	−26.09	2238 ± 32	2162–2329	2231
TERRA-120310a29	YXI08	140	−26.28	3088 ± 32	3265–3361	3312
TERRA-113010b15	YXI09	193	−26.47	3487 ± 43	3703–3828	3763
TERRA-113010b16	YXI10	201	−25.74	3613 ± 47	3860–3980	3925
TERRA-120310a17	YXI11	240	−26.07	3884 ± 29	4259–4407	4329
TERRA-113010b17	YXI12	283	−26.01	6435 ± 48	7323–7419	7360
TERRA-113010b18	YXI13	335	−24.70	7268 ± 50	8021–8160	8090
TERRA-120310a27	YXI14	383	−25.07	7762 ± 35	8481–8591	8544
TERRA-113010b19	YXI15	411	−25.03	9114 ± 47	10,220–10,370	10,265
TERRA-113010b20	YXI16	442	−25.58	9668 ± 57	10,874–11,194	11,074
TERRA-113010b21	YXI17	485	−24.58	10,470 ± 46	12,226–12,543	12,425
TERRA-113010b22	YXI18	518	−24.88	10,808 ± 40	12,614–12,729	12,681
TERRA-120310a15	YXI19	539	−25.25	12,473 ± 49	14,243–14,887	14,598
TERRA-120310a20	YXI20	608	−24.59	14,390 ± 51	17,247–17,660	17,506
TERRA-113010b23	YXI21	636	−24.68	15,412 ± 64	18,576–18,708	18,650
TERRA-120310a22	YXI22	757	−24.82	17,594 ± 69	20,903–21,258	20,974
TERRA-120310a21	YXI23	768	−24.48	18,838 ± 65	22,294–22,511	22,421
TERRA-121610a13	YXI24	796	−24.16	20,030 ± 110	23,757–24,163	23,937
TERRA-113010b26	YXI25	805	−24.44	21,015 ± 92	24,884–25,254	25,063
TERRA-120310a11	YXI26	819	−24.60	22,093 ± 83	26,269–26,694	26,503
TERRA-113010b27	YXI27	835	−24.42	22,697 ± 95	27,016–27,774	27,398
TERRA-113010b29	YXI28	912	−24.53	24,844 ± 119	29,461–29,868	29,698
TERRA-120310a18	YXI29	1010	−24.25	28,814 ± 126	33,046–33,504	33,303

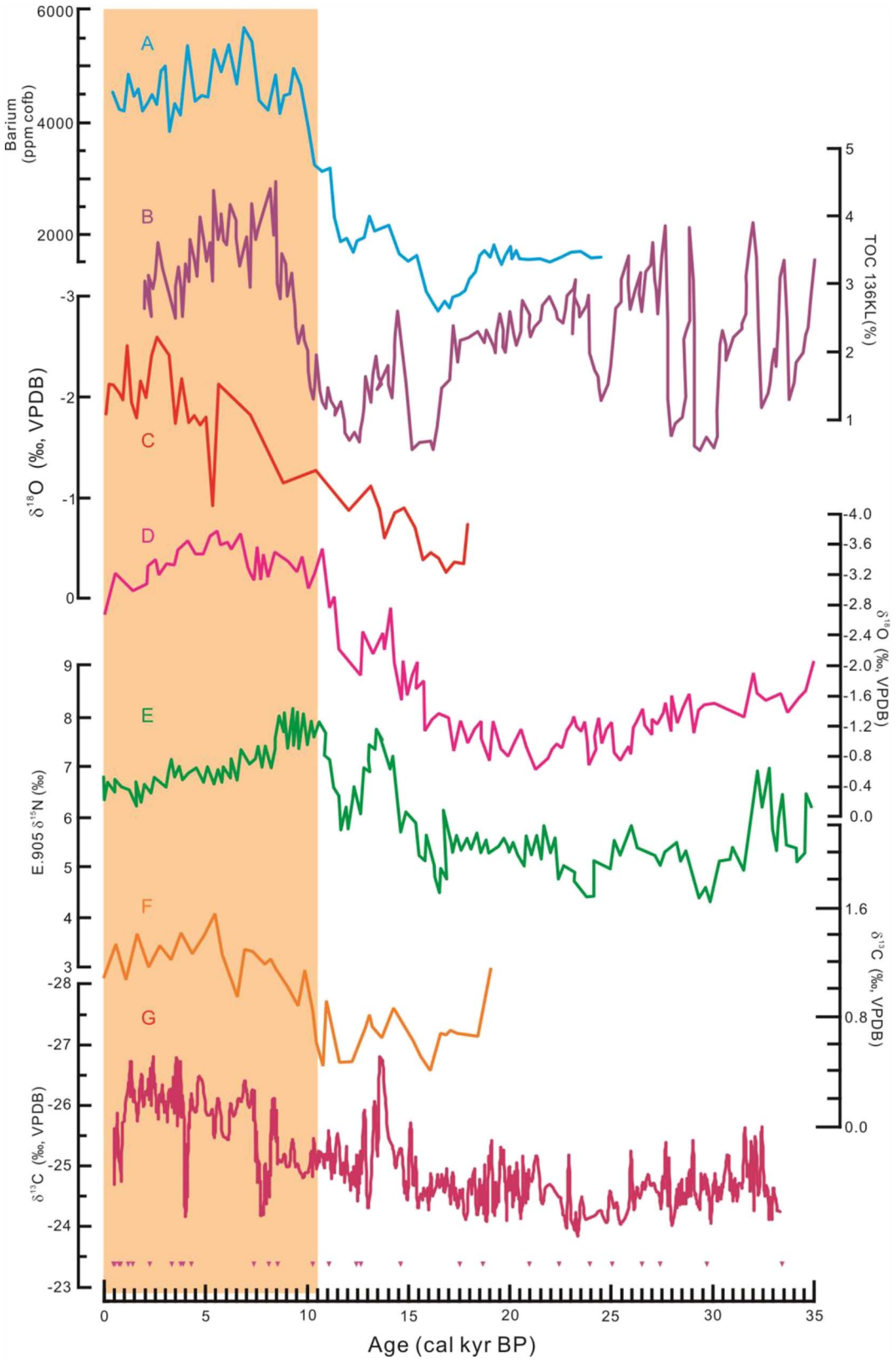

Fig. 3. Secular change trends of the India summer monsoon intensity inferred from multiple proxies in the period from the late Last Glacial to the Holocene. (A) The barium content in sediment core 74 KL in the western Arabian Sea (Site 10 in Fig. 1; Sirocko et al., 1993). (B) The content of total organic carbon in sediment core 136 KL in the northern Arabian Sea (Site 8 in Fig. 1; Schulz et al., 1998). (C) The $\delta^{18}O$ record of *Globigerinoides sacculifer* in sediment core GC-5 in the eastern Arabian Sea (Site 7 in Fig. 1; Thamban et al., 2001). (D) The $\delta^{18}O$ record of *Globigerina ruber* in sediment core KL 126 in the northern Bay of Bengal (Site 6 in Fig. 1; Kudrass et al., 2001). (E) The $\delta^{15}N$ record of sediment core 905 in the western Arabian Sea (Site 12 in Fig. 1; Ivanochko et al., 2005). (F) The $\delta^{13}C$ record of *Globigerina ruber* in sediment core 4018G in the western Arabian Sea (Site 11 in Fig. 1; Tiwari et al., 2010). (G) The $\delta^{13}C$ record of Baoan peat cellulose at the southeastern edge of the Tibetan Plateau (Site 1 in Fig. 1; this study). The red triangles at the bottom indicate the calibrated ^{14}C age-control points used to construct the age model of the Baoan peat core. The shadow shows the monsoon changes during the Holocene.

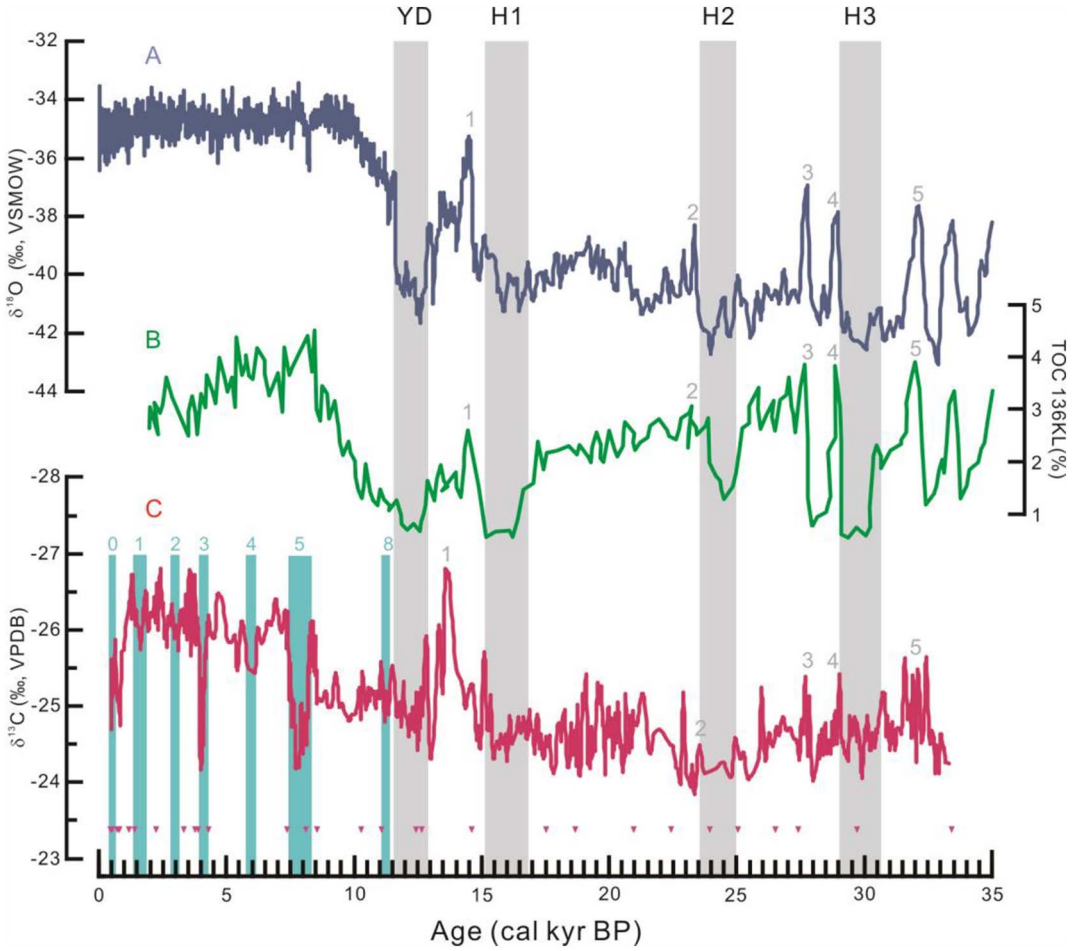

Fig. 4. The responses of the India summer monsoon (ISM) to the northern high latitude climate. (A) Temperature record reconstructed from the $\delta^{18}O$ of the GISP2 ice core (Stuiver and Grootes, 2000). (B) The ISM wind intensity record reconstructed from the total organic carbon content in sediment core 136 KL in the northern Arabian Sea (Site 8 in Fig. 1; Schulz et al., 1998). (C) The ISM precipitation record reconstructed from the $\delta^{13}C$ of Baoan peat cellulose (Site 1 in Fig. 1; this study). The climatic intervals are abbreviated as follows: YD–Younger Dryas; H1–3–Heinrich events 1–3. The gray bars indicate the YD and Heinrich events and the responses of the ISM. The gray numbers (1–5) indicate Greenland Interstadials and correlated events in the ISM. The blue numbers (0–5, 8) and bars indicate the ice rafted debris (IRD) events in the North Atlantic Ocean during the Holocene (Bond et al., 1997) and the responses of the ISM. The red triangles at the bottom indicate the calibrated ^{14}C age-control points used to construct the age model of the Baoan peat core. (For interpretation of the references to color in this figure legend, the reader is referred to the web version of this article.)

interpreted as reflecting fluctuations in the intensity of ISM-induced biological productivity. The high TOC content reflects increased biological productivity induced by strong winds of the ISM and vice versa (Schulz et al., 1998). Therefore, the close correlation shown by curves A and B in Fig. 4 reflects the correlation between the wind intensity of the ISM and the high northern latitude climate. Strong ISM winds correlate with interstadial climate events in the northern North Atlantic region. In contrast, periods of low ISM wind intensity are associated with intervals of atmospheric cooling events in the northern high latitudes (Schulz et al., 1998). Since summer monsoon wind intensity and summer monsoon rainfall are meteorologically seen as the two basic attributes of monsoon activity and are usually used individually or together to indicate the intensity of the summer monsoon (Huang and Huang, 1999), it can be inferred that if the strong correlation between the ISM and the high northern latitude climate revealed by the ISM wind intensity record is an objective natural phenomenon, then it should also be reflected in the ISM rainfall record, as long as the record has sufficient precision of ^{14}C age constraints as well as sufficient sensitivity. However, such a summer monsoon rainfall proxy record has not yet emerged within the continental area.

Fig. 4 shows the comparison between two proxy records of the ISM rainfall and winds. Corresponding to the abrupt cooling and warming events in the high northern latitudes during the late Glacial and the last deglaciation, respectively, the monsoon rainfall inferred from the peat cellulose $\delta^{13}C$ (Fig. 4C) and the wind inferred from the TOC content (Fig. 4B) show synchronous changes. In the B/A warm period from approximately 14.7 to 13.3 cal kyr BP, there seems to be a slight mismatch between the two peak times of monsoon rainfall and winds. The former corresponds to the Allerød warm period, and the latter corresponds to the Bølling warm period, which has led to some discussion (Hong et al., 2014b; Nag and Phartiyal, 2015). However, the monsoon rainfall and wind intensity both show an enhancement during the B/A warm period in general.

The correlation noted above suggests the existence of two simultaneous physical-biological processes associated with the millennial-scale ISM activity. When strong ISM winds led to high biological productivity in the OMZ along the continental margin off Pakistan in the northeastern Arabian Sea, heavy ISM rainfall was synchronously leading to opening of C3 plant leaf stomata in the Hengduan Mountains at the southeastern edge of the Tibetan Plateau, which resulted in the occurrence of lower $\delta^{13}C$ values in the local C3 plants. The above two processes are consistent in time with the abrupt warming events in the high northern latitudes. In contrast, corresponding to the abrupt cooling events of the high northern latitudes, the weakened ISM winds led to the low TOC content in sediments from the OMZ, while slight ISM rainfall synchronously caused closing of C3 plant leaf stomata in the Baoan peatland, which resulted in the occurrence of higher $\delta^{13}C$ values in the local C3 plants. Thus, our Baoan peat record for the first time

provides additional evidence for the correlation between the ISM and the high northern latitude climate, which shows that both ISM rainfall and winds can indicate this teleconnection. In addition, the close correlations between the above-noted three climate parameters, including ISM rainfall inferred from the Baoan peat cellulose $\delta^{13}C$ value, ISM winds intensity inferred from the TOC content in sediment in the OMZ from off Pakistan, and atmospheric temperature inferred from the $\delta^{18}O$ values in the GISP2 ice core, show a one-to-one teleconnection between them. This one-to-one correlation may imply the existence of a common dominant factor for the climate changes in the late Last Glacial and last deglaciation.

3.2.2. Millennial-scale variability of ISM intensity during the Holocene

Unlike the TOC record in the OMZ from off Pakistan that reflects only the abrupt variation of the ISM during the Last Glacial and last deglaciation, the Baoan peat cellulose $\delta^{13}C$ time series also provides the millennial-scale variability of the ISM intensity during the Holocene. Fig. 4C shows an abrupt change spectrum of the ISM from the late Last Glacial to the Holocene, which provides new opportunities for better understanding of the characteristics of the ISM abrupt variation during the cold Last Glacial and warm Holocene.

Previous studies have revealed nine abrupt cooling events recorded in ice-rafted debris (IRD) sediment in the North Atlantic Ocean during the Holocene (Bond et al., 1997). A temperature oscillation denoted by these cooling events is usually known as a “Bond event” or a “Bond cycle” (Wanner et al., 2011). This discovery by Bond et al. (1997, 2001) stimulated the study of abrupt climate changes in the Holocene and gave rise to a large number of publications. In 2003 alone, three proxy records for the ISM from the Eastern Arabian Sea (Gupta et al., 2003), Southern Oman (Fleitmann et al., 2003), and the southeastern Tibetan Plateau (Hong et al., 2003) reported abrupt weakening phenomena of the ISM corresponding to the IRD events. However, it has also been noted that the correlation has nonlinear characteristics. The Bond events corresponding to weakened monsoons, for instance, are 1, 3, 4, 6, and 7 in the Eastern Arabian Sea (Gupta et al., 2003); 2, 3, 4, 5, and 6 in Southern Oman (Fleitmann et al., 2003); and 1, 3, 5, 7, and 8 in the southeastern Tibetan Plateau (Hong et al., 2003) (also see Table 1 of Wanner et al., 2011). In the case of the Baoan peat record, the events corresponding to the weakened monsoon are 0, 1, 2, 3, 4, 5, and 8 (Fig. 4C). Based on 30 papers published since 1995, Wanner et al. (2011) suggested that “According to the review in Table 1, the cycles 2 (peak at ~3 kyr BP) and 5 (showing a peak 5a at ~7.5 and a peak 5b at ~8.5 kyr BP) are referred to most commonly” (page 3111 in Wanner et al., 2011). To date, there has been no ISM proxy record that fully shows the one-to-one correspondence between the weakened monsoon and the Bond event during the Holocene. These dissimilar responses shown by the various proxy indicators from different regions highlight the complexity of the relationship between the low latitude monsoon and the high northern latitude climate during the Holocene.

In addition, corresponding to the cooling events in the high northern latitudes, the Baoan peat shows a total of 11 abrupt weakening events for the ISM, of which four occurred in the cold stages (the late Last Glacial and last deglaciation) and the other seven occurred in the warm stage (the Holocene) (Fig. 4C). It is worth noting that the decline amplitudes inferred from the Baoan peat cellulose $\delta^{13}C$ values are markedly different. The amplitudes of the abrupt decreases in the cold stages are smaller and in the warm stage are larger in general. In climate science, the following three criteria are often used to classify events as extreme, that they occur with relatively low frequency/rate,have large magnitude deviations from the norm, and often result in large socio-economic losses (Beniston et al., 2007). According these criteria, extreme events in the history of the ISM intensity change can be identified for further investigation. The three abrupt weakening events corresponding to the Bond events 5 (peak value at ~8 cal kyr BP), 3 (peak value at ~4 cal kyr BP), and 0 (peak value at ~0.5 cal kyr BP) are probably the extremely weakened events in the ISM during the past 33,300 years (Fig. 4C). Their $\delta^{13}C$ values abruptly increase by approximately 2.0‰, 2.3‰, and 2.1‰, respectively, which are clearly greater than the average increase value (approximately 1.1‰) of other weakening events, including the YD event (1.5‰), H1 (0.88‰), H2 (1.0‰), and H3 (1.1‰). These results may suggest that the extremely weakened events in the ISM often occurred during warm stages in geological history. On the other hand, the climate condition during the last deglaciation, located in the transition from the cold stage to the warm stage, also shows great fluctuations (Fig. 4C). The abrupt strengthening of the ISM occurred in the B/A warming period (Wang et al., 2001; Dykoski et al., 2005; Hong et al., 2014b), which implies that the extremely strengthened events of the ISM cannot be ruled out in the present warming period.

The Baoan peat $\delta^{13}C$ record highlights a phenomenon that ISM anomalies, including the extreme weakening and strengthening, tend to occur in the warm stages during the past 33,300 years, although that compared to the contemporary warming, the impact of human activity was small at that time. This result may provide a historical scenario for understanding the modern climate variation and possible impacts. For instance, corresponding to the Bond event 3, the ISM intensity inferred from the Baoan peat cellulose $\delta^{13}C$ value abruptly decreased during the period from approximately 4.3 to 3.8 cal kyr BP with the maximum $\delta^{13}C$ peak value centered at 4.0 cal kyr BP, which is consistent with previous results from other proxy records for the ISM (Cullen et al., 2000; Thompson et al., 2002; Hong et al., 2003; Arz et al., 2006; Berkelhammer et al., 2012) (Fig. 5). This extreme weakening event has been termed the “4-ka event” (Weiss et al., 1993; Perry and Hsu, 2000), or “4.2-ka event” (Staubwasser et al., 2003; Booth et al., 2005), or “Holocene Event 3” (Bond et al., 1997; deMenocal, 2001). The severe drought caused by this extreme climate event covered widespread areas from East Africa through the subcontinent of India and the Tibetan Plateau (Berkelhammer et al., 2012) and eastward toward southeastern China (Wu and Liu, 2004). At approximately the same time, once-prosperous ancient civilizations in Egypt, Indus, and Mesopotamia unexpectedly declined. Although the reasons leading to the decline of ancient civilizations are likely to be complex, the destructive impacts of this extreme climate on the civilizations have still been acknowledged by many paleoclimatologists (Weiss et al., 1993; Weiss and Raymond, 2001; Perry and Hsu, 2000; deMenocal, 2001; Staubwasser et al., 2003; Wu and Liu, 2004; Berkelhammer et al., 2012). Some recent studies show that fluctuations in climate have highly significant influence on modern agriculture of India (Turner and Annamalai, 2012; Bollasina, 2014; Singh et al., 2014). Abnormally high temperatures and drought increase suicide rates of Indian farmers during India's agricultural growing season, when heat also lowers crop yields, but suicide rates decrease as the ISM precipitation increases (Carleton, 2017). Irrespective of contemporary climate warming, whether there will be natural extreme monsoon changes, including extreme weakening and strengthening, is still worthy of investigation. How to recognize the relative contributions of anthropogenic activities and natural effects on monsoon variability remains a major challenge.

3.2.3. Possible reasons for respective characteristics of the ISM in the Holocene and the late Last Glacial

An abrupt change of the ISM, as discussed in this study, usually refers to a sudden monsoonal shift corresponding to a rapid climate change event in the high northern latitude region (Overpeck and Webb, 2000; Gupta et al., 2003; Fleitmann et al., 2003; Hong et al., 2003; Wanner et al., 2011). Therefore, the dynamics of an abrupt ISM shift should be closely related to the dynamics of the sudden climate change event in the high northern latitude region. It has been known that the reasons for abrupt climate changes in the high northern latitudes during the Last Glacial versus the Holocene vary greatly (Bond et al., 1997). For more than 20 years, observations and modeling have demonstrated that the existence of the Northern Hemisphere large ice sheet and its instability are the dominant reasons for abrupt climate changes in the

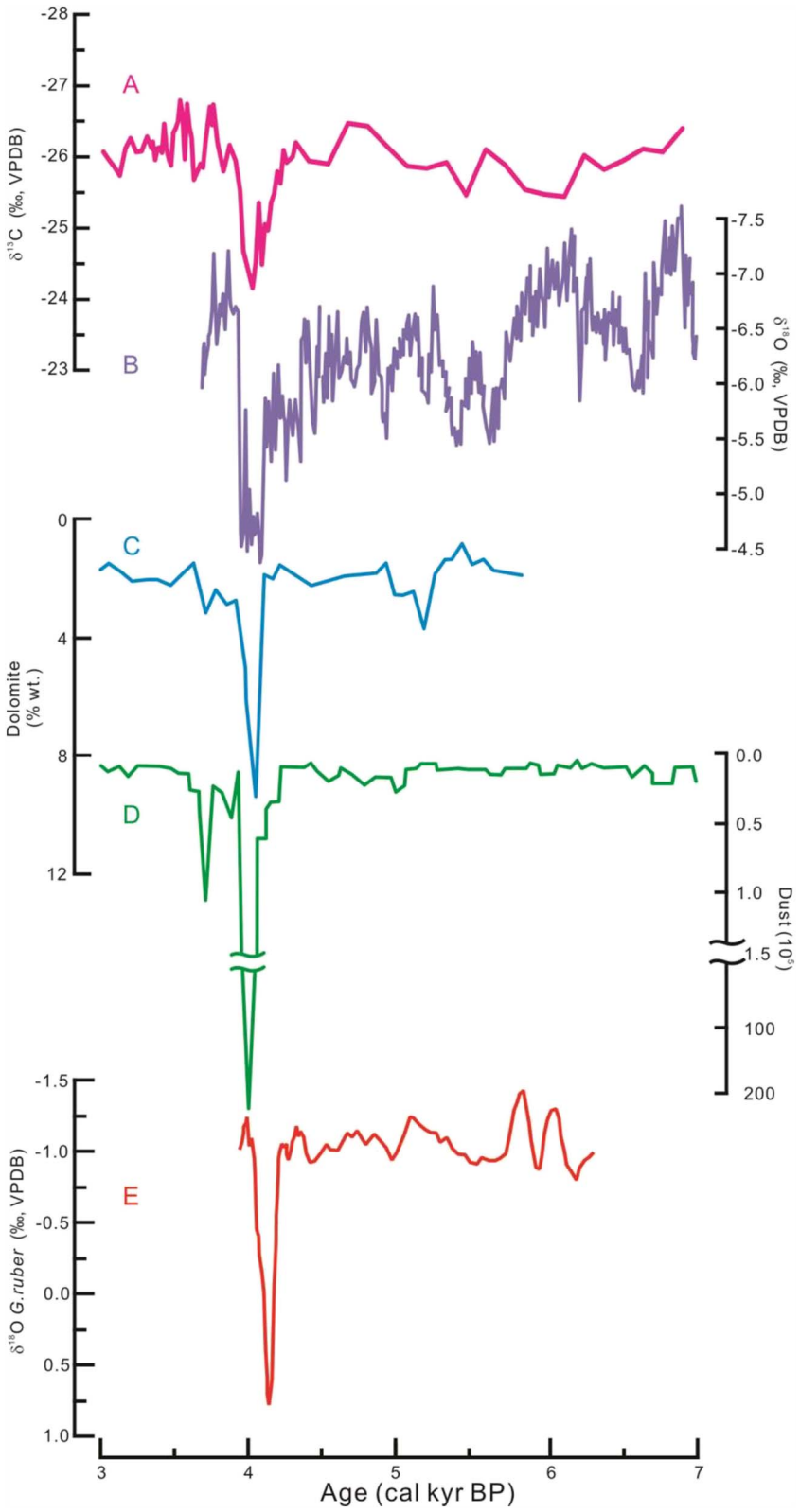

Fig. 5. The abrupt changes of the India summer monsoon at about 4 cal kyr BP inferred from multiple proxies. (A) The $\delta^{13}C$ values of Baoan peat cellulose (this study). (B) The $\delta^{18}O$ values of stalagmites from Mawmluh Cave (Berkelhammer et al., 2012). (C) The dolomite content in sediment core M5-422 in Gulf of Oman (Cullen et al., 2000). (D) The dust content in the Kilimanjaro's ice core (Thompson et al., 2002). (E) The $\delta^{18}O$ values of *Globigerinoides rubber* in sediment core GeoB 5836-2 in the northern Red Sea (Arz et al., 2006).

Last Glacial. The ocean conveyor theory of Broecker et al. (1985) has asserted that when cross-equatorial ocean water flows toward the North Atlantic Ocean and reaches high latitudes, the increasing salinity of seawater results in its descending into the deep ocean and forming the deep-layer water that flows back south, thereby completing the important Atlantic meridional overturning circulation (AMOC). When much fresh meltwater enters the North Atlantic Ocean, the seawater at high latitudes is freshened abruptly, and the AMOC slows down or even stops, resulting in a large decrease of northward heat transfer and the precipitous cooling of the North Atlantic region (Broecker, 1994a, 1994b, 1997; Knutti et al., 2004; EPICA Community Members, 2006; Barker et al., 2009; Chiang and Friedman, 2012; Landais et al., 2015). This hypothesis not only illustrates the mechanism of the abrupt cooling events that occurred in the high northern latitude in the Last Glacial

and deglaciation periods but has also been used to explain the abrupt cooling event that occurred in the early Holocene (Teller et al., 2002; Clarke et al., 2004; Alley and Agustsdottir, 2005). The mechanism linking these changes and the ISM is a widely accepted hypothesis that these changes were also accompanied by south-north shifts in the mean latitude position of the Intertropical Convergence Zone (ITCZ) and the weakening-strengthening variations of the ISM intensity (Broccoli et al., 2006; Broecker, 2006; Clement and Peterson, 2008; Chiang and Friedman, 2012).

The factors that affect the high northern latitude climate and the ISM abrupt changes are more diverse during the Holocene. Bond et al. (1997) noted that the large ice sheet in the Northern Hemisphere has clearly retreated in the Holocene and that sudden millennial-scale climate changes in the Holocene should operate differently from those in glacial periods. Abrupt temperature changes appear to have been influenced by variations in solar output through the entire Holocene (van Geel et al., 1998; Chambers et al., 1999; Beer et al., 2000; Hong et al., 2000; Bond et al., 2001; Wanner et al., 2008; Gray et al., 2010). This hypothesis has also affected the study of the ISM. When the teleconnection between the ISM and the high northern latitude climate during the Holocene was discovered, changes in solar activity were proposed as the main driving factors (Fleitmann et al., 2003; Dykoski et al., 2005; Wang et al., 2005). In addition, the impacts of the sea surface temperature (SST) gradient variation between the high and low latitudes resulting from the ocean thermohaline circulation shift and the El Niño-Southern Oscillation (ENSO) variations on the ISM have also been discussed (Hong et al., 2003). The discussions noted above are summarized in a conceptual model by Hong et al. (Fig. 6 of Hong et al., 2009). The model suggests it is important that the sudden temperature decreases are always accompanied by abrupt declines in the ISM, whether because of weakened solar activity or reduced meltwater discharge. The influences of weakened solar activity and reduced meltwater discharge on the climate could be compounded. Reduced solar activity and meltwater outburst both appear to act as triggers for occurrence of the ENSO phenomenon in the equatorial Pacific Ocean, which may result in broad teleconnections between the temperature anomaly in the high northern latitudes and abrupt variation of the ISM (Hong et al., 2009). Based on a comprehensive analysis of large amounts of temperature and humidity/precipitation data from official data repositories and scientific journals, Wanner et al. (2011) suggested that, most likely, decreasing solar insolation combined with a possible slowdown of the thermohaline circulation and, in some cases, also with a series of tropical volcanic eruptions, may lead to Northern Hemisphere cooling, a southern shift of the ITCZ and a weakening of the ISM in the Holocene. The studies noted above show that the factors affecting abrupt climate change during the Holocene are more complex than those during the late Last Glacial and last deglaciation. It is not yet known how to quantitatively identify the relative contributions of these factors (solar activity, thermohaline circulation, ENSO, volcano activities, etc.) to the abrupt variations of temperature, monsoon rainfall, and the ITCZ in the Holocene and the temporal and spatial changes of these contributions. These uncertainties possibly result in a nonlinear correlation between the ISM and the abrupt climate changes in high northern latitudes during the Holocene.

On the other hand, the effects of these factors may be superimposed. We consider that once these factors or some of the factors simultaneously appear in a certain time and place, they may eventually constitute a stronger combined effect than any single factor, although the relative importance of each is unclear. Diversification of influencing factors may be the reason why extreme climate events occur more frequently in the Holocene epoch than in the glacial stage. Fig. 4C shows, for instance, that there is one significant temperature anomaly at approximately 8 cal kyr BP in the $\delta^{18}O$ record of the GISP2 ice core, which has been termed the “8-ka event” or “8.2-ka event” (Alley and Agustsdottir, 2005). It is estimated that by then the temperature had cooled by approximately 6 °C in the broad Northern Hemisphere region (Alley and Agustsdottir, 2005). This cooling extent is roughly the same as that of the Heinrich event (approximately 5 °C, Bard et al., 2000) but slightly smaller than the cooling range of the YD event (approximately 8 °C, Dansgaard et al., 1989). The occurrences of these cooling events have often been attributed to meltwater outflows into the North Atlantic Ocean and slowdowns of the AMOC (Alley and Agustsdottir, 2005). As noted before, our Baoan peat cellulose $\delta^{13}C$ record clearly shows that the amplitude of the decline in the ISM for the 8-ka event was significantly greater than those for the Heinrich and the YD events (Fig. 4C). This phenomenon clearly cannot be explained by a single meltwater flood mechanism; instead, it provides support for the hypothesis of superposition of multiple factors during the Holocene. In particular, the 4-ka event shown in the Baoan peat cellulose $\delta^{13}C$ record is likely to be another example of a combination of several internal and external factors, since the Northern Hemisphere large ice sheet has clearly retreated, and the effect of meltwater floods has been small at that time. As to the potential factors affecting the 4-ka event, several physical processes have been advocated by scientists or recorded by relevant time series, for instance, reduced solar activity (Bond et al., 2001; Müller et al., 2006; Vonmoos et al., 2006), changes in the thermohaline circulation (Bianchi and McCave, 1999; deMenocal et al., 2000; Hong et al., 2003), Neoglacial glacier advances (Winkler and Matthews, 2010; Wanner et al., 2011), volcanic eruptions (deMenocal et al., 2001; Wanner et al., 2008), El Niño activity (Moy et al., 2002; Koutavas et al., 2006; Hong et al., 2009), etc. The superposition of the effects of these potential processes likely resulted in the dramatic decrease of the ISM intensity at approximately 4 cal kyr BP (Figs. 4C and 5).

4. Conclusions

(1) We present a 33,300-year stable carbon isotopic ($\delta^{13}C$) time series of Baoan peat cellulose. It records the continuous change history of the ISM intensity from the late Last Glacial to the Holocene. It is also rare in showing the respective characteristics of the ISM variability during the cold late Last Glacial and the warm Holocene stages.

(2) On the glacial-interglacial timescale, the ISM is generally weaker in the cold stage and stronger in the warm stage. In addition, corresponding to the abrupt millennial-scale climate changes in the high northern latitudes, the ISM shows a series of sudden millennial-scale variations. The abrupt variations appear in both the cold stage and the warm stage. These results provide new evidence for the response relationship of the ISM to climate changes in the high northern latitudes.

(3) This response relationship may behave differently in the cold stage and warm stage. The response in the cold stage seems to be one-to-one. When the YD event and the Heinrich events occurred in the high northern latitudes, the ISM abruptly decreased. In contrast, when the abrupt warming events, including the B/A event and D/O events or oscillations 2, 3, 4, and 5, occurred in the high northern latitudes, the ISM abruptly strengthened. However, the response relationship in the warm Holocene stage is mainly manifested in the abrupt weakening of the ISM, and the latter often shows partial responses to the abrupt cooling events in the high northern latitude region.

(4) The Baoan peat record indicates that the amplitude of the abrupt variation of the ISM intensity is generally larger in the warm stage than in the cold stage. Extreme change events in the ISM intensity occurred much more during the warm stage, although the impact of human activities was still small at that time. These results provide historical background for evaluating concerns over contemporary and future climate change.

(5) We consider that the dissimilar characteristics of the ISM abrupt changes in the warm stage and cold stage may result from different combinations of climatic forcing factors, respectively. Compared

with the mechanism dominated by the meltwater outflow and thermohaline circulation change in the cold stage, the factors affecting ITCZ migration are more diverse in the warmer stages. The superposition of the effects of various driving factors and its changes in time and space may be the basic cause of the random occurrence of the ISM extreme change events in the warm stage.

Author contributions

B.H. and Y.H. designed research; B.H., M.U., H.Y., H.P., M.K. and W.D. performed research; B.H. and Y.H. analyzed data and wrote the paper.

The authors declare no conflict of interest

Acknowledgments

This work was supported by the National Natural Science Foundation of China (Grant Nos. 41373134, 41173127, 41773140).

References

Alley, R.B., Agustsdottir, A.M., 2005. The 8k event: cause and consequences of a major Holocene abrupt climate change. Quat. Sci. Rev. 24, 1123–1149.
Amesbury, M.J., Charman, D.J., Newnham, R.M., Loader, N.J., Goodrich, J.P., Royles, J., Campbell, D.I., Roland, T.P., Gallego-Sala, A., 2015. Carbon stable isotopes as a palaeoclimate proxy in vascular plant dominated peatlands. Earth Planet. Sci. Lett. 164, 161–174.
An, Z.S., Clemens, S.C., Shen, J., Qiang, X.K., Jin, Z.D., Sun, Y.B., Prell, W.L., Luo, J.J., Wang, S.M., Xu, H., Cai, Y.J., Zhou, W.J., Liu, X.D., Liu, W.G., Shi, Z.G., Yan, L.B., Xiao, X.Y., Chang, H., Wu, F., Ai, L., Lu, F.Y., 2011. Glacial-interglacial Indian summer monsoon dynamics. Science 333, 719–723.
Arz, H., Lamy, F., Patzold, J., 2006. A pronounced dry event recorded around 4.2 ka in brine sediments from the northern Red Sea. Quat. Res. 66, 432–441.
Bard, E., Rostek, R., Turon, J.-L., Gendreau, S., 2000. Hydrological impact of Heinrich events in the subtropical northeast Atlantic. Science 289, 1321–1324. http://dx.doi.org/10.1126/science.289.5483.1321.
Barker, S., Diz, P., Vautravers, M.J., Pike, J., Knorr, G., Hall, I.R., Broecker, W.S., 2009. Interhemispheric Atlantic seesaw response during the last deglaciation. Nature 457, 1097–1102.
Beer, J., Mende, W., Stellmacher, R., 2000. The role of the sun in climate forcing. Quat. Sci. Rev. 19, 403–415.
Beniston, M., Stephenson, D.B., Christensen, O.B., Ferro, C.A.T., Frei, C., Goyette, S., Halsnaes, K., Holt, T., Jylhä, K., Koffi, B., Palutikof, J., Schöll, R., Semmler, T., Woth, K., 2007. Future extreme events in European climate: an exploration of regional climate model projections. Clim. Chang. 81, 71–95. http://dx.doi.org/10.1007/s10584-006-9226-z.
Berkelhammer, M., Sinha, A., Stott, L., Cheng, H., Pausata, F.S.R., Yoshimura, K., 2012. An Abrupt Shift in the Indian Monsoon 4000 Years Ago. Climates, Landscapes, and Civilizations. AGU Geophysical Monograph Series 198. pp. 75–87. http://dx.doi.org/10.1029/2012gm/001207.
Bianchi, G.G., McCave, I.N., 1999. Holocene periodicities in North Atlantic climate and deep-ocean flow south of Iceland. Nature 397, 515–517.
Bollasina, M.A., 2014. Probing the monsoon pulse. Nat. Clim. Chang. 4, 422–423.
Bond, G., Showers, W., Cheseby, M., Lotti, R., Almasi, P., deMenocal, P., Priore, P., Cullen, H., Hajdas, I., Bonani, G., 1997. A pervasive millennial-scale cycle in North Atlantic Holocene and glacial climates. Science 278, 1257–1266.
Bond, G., Kromer, B., Beer, J., Muscheler, R., Evans, M.N., Showers, W., Hoffmann, S., Lotti-Bond, R., Hajdas, I., Bonani, G., 2001. Persistent solar influence on North Atlantic climate during the Holocene. Science 294, 2130–2136.
Booth, R.K., Jackson, S.T., Forman, S.L., Kutzbach, J.E., Bettis, E.A., Kreig, J., Wright, D.K., 2005. A severe centennial-scale drought in mid-continental North America 4200 years ago and apparent global linkages. The Holocene 15, 321–328.
Briggs, D.E.G., Evershed, R.P., Lockheart, M.J., 2000. The biomolecular paleontology of continental fossils. Paleobiology 26, 169–193.
Broccoli, A.J., Dahl, K.A., Stouffer, R.J., 2006. Response of the ITCZ to Northern Hemisphere cooling. Geophys. Res. Lett. 33, L01702. http://dx.doi.org/10.1029/2005GL024546.
Broecker, W.S., 1994a. Ocean circulation - an unstable superconveyor. Nature 367, 414–415.
Broecker, W.S., 1994b. Massive iceberg discharges as triggers for global climate change. Nature 372, 421–424.
Broecker, W.S., 1997. Thermohaline circulation, the Achilles heel of our climate system: will man-made CO_2 upset the current balance. Science 278, 1582–1588.
Broecker, W.S., 2006. Abrupt climate change revisited. Glob. Planet. Chang. 54, 211–215. http://dx.doi.org/10.1016/j.gloplacha.2006.06.019.
Broecker, W.S., Peteet, D.M., Rind, D., 1985. Does the ocean-atmosphere system have more than one stable mode of operation? Nature 315, 21–26.
Carleton, T.A., 2017. Crop-damaging temperatures increase suicide rates in India. PNAS 114, 8746–8751.
Chambers, F.M., Ogle, M.I., Blackford, J.J., 1999. Palaeoenvironmental evidence for solar forcing of Holocene climate: linkages to solar science. Prog. Phys. Geogr. 23, 181–204.
Chambers, F.M., Booth, R.K., De Vleeschouwer, F., Lamentowicz, M., Le Roux, G., Mauquoy, D., Nichols, J.E., van Geel, B., 2012. Development and refinement of proxy-climate indicators from peats. Quat. Int. 268, 21–33.
Chiang, J.C.H., Friedman, A.R., 2012. Extratropical cooling, interhemispheric thermal gradients, and tropical climate change. Annu. Rev. Earth Planet. Sci. 40, 383–412.
Clarke, G.K.C., Leverington, D.W., Teller, J.T., Dyke, A.S., 2004. Paleohydraulics of the last outburst flood from glacial Lake Agassiz and the 8200 BP cold event. Quat. Sci. Rev. 23, 389–407.
Clemens, S.C., Prell, W.L., 1990. Late Pleistocene variability of Arabian Sea summer monsoon winds and continental aridity: eolian records from the lithogenic component of deep-sea sediments. Paleoceanography 5, 109–145.
Clemens, S.C., Prell, W.L., 2003. A 350,000 year summer-monsoon multiproxy stack from the Owen Ridge, Northern Arabian Sea. Mar. Geol. 201, 35–51.
Clemens, S.C., Prell, W.L., 2007. The timing of orbital-scale Indian monsoon changes. Quat. Sci. Rev. 26, 275–278.
Clemens, S.C., Prell, W.L., Murray, D., Shimmield, G., Weedon, G., 1991. Forcing mechanisms of the Indian Ocean monsoon. Nature 353, 720–725.
Clemens, S.C., Murray, D.W., Prell, W.L., 1996. Nonstationary phase of the Plio-Pleistocene Asian monsoon. Science 274, 943–948.
Clement, A.C., Peterson, L.C., 2008. Mechanisms of abrupt climate change of the last glacial period. Rev. Geophys. 46, RG4002. http://dx.doi.org/10.1029/2006RG000204.
Coplen, T.B., 2011. Guidelines and recommended terms for expression of stable-isotope-ratio and gas-ratio measurement results. Rapid Commun. Mass Spectrom. 25 (17), 2538–2560.
Cullen, H., deMenocal, P., Hemming, S., Hemming, G., Brown, F., Guilderson, T., Sirocko, F., 2000. Climate change and the collapse of the Akkadian empire: evidence from the deep sea. Geology 28, 379–382.
Dansgaard, W., White, J.W.C., Johnsen, S.J., 1989. The abrupt termination of the Younger Dryas climate event. Nature 339, 532–533.
Dansgaard, W., Johnsen, S.J., Clausen, H.B., Dahl-Jensen, D., Gundestrup, N.S., Hammer, C.U., Hvidberg, C.S., Steffensen, J.P., Sveinbjornsdottir, A.E., Jouzel, J., Bond, G., 1993. Evidence for general instability of past climate from a 250 ka ice-core record. Nature 364, 218–220.
deMenocal, P.B., 2001. Cultural responses to climate change during the Late Holocene. Science 292, 667–673.
deMenocal, P.B., Ortiz, J., Guilderson, T., Sarnthein, M., 2000. Coherent high- and low-latitude climate variability during the Holocene warm period. Science 288, 2198–2202.
Deplazes, G., Lückge, A., Stuut, J.B.W., Pätzold, J., Kuhlmann, H., Husson, D., Fant, M., Haug, G.H., 2014. Weakening and strengthening of the Indian monsoon during Heinrich events and Dansgaard-Oeschger oscillations. Paleoceanography 29, 99–114.
Diefendorf, A.F., Mueller, K.E., Wing, S.L., Koch, P.L., Freeman, K.H., 2010. Global patterns in leaf ^{13}C discrimination and implications for studies of past and future climate. PNAS 107, 5738–5743.
Dykoski, C.A., Edwards, R.L., Cheng, H., Yuan, D.X., Cai, Y.J., Zhang, M.L., Lin, Y.S., Qing, J.M., An, Z.S., Revenaugh, J., 2005. A high-resolution absolute-dated Holocene and deglacial Asian monsoon record from Dongge Cave, China. Earth Planet. Sci. Lett. 233, 71–86.
EPICA Community Members, 2006. One-to-one coupling of glacial climate variability in Greenland and Antarctica. Nature 444, 195–198.
Farquhar, G.D., Ehleringer, J.R., Hubick, K.T., 1989. Carbon isotope discrimination and photosynthesis. Annu. Rev. Plant Physiol. Plant Mol. Biol. 40, 503–537.
Fleitmann, D., Burns, S.J., Mudelsee, M., Neff, U., Kramers, J., Mangini, A., Matter, A., 2003. Holocene forcing of the Indian monsoon recorded in a stalagmite from Southern Oman. Science 300, 1737–1739.
Francey, R.J., Farquhar, G.D., 1982. An explanation of $^{13}C/^{12}C$ variations in tree rings. Nature 297, 28–31.
Gray, L.J., Beer, J., Geller, M., Haigh, J.D., Lockwood, M., Matthes, K., Cubasch, U., Fleitmann, D., Harrison, G., Hood, L., Luterbacher, J., Meehl, G.A., Shindell, D., van Geel, B., White, W., 2010. Solar influences on climate. Rev. Geophys. 48, RG4001. http://dx.doi.org/10.1029/2009RG000282.
Green, J.W., 1963. Wood cellulose. In: Whistler, R.L. (Ed.), Methods in Carbohydrate Chemistry. 3. Academic Press, New York, pp. 9–22.
Gupta, A.K., Anderson, D.M., Overpeck, J.T., 2003. Abrupt changes in the Asian southwest monsoon during the Holocene and their links to the North Atlantic Ocean. Nature 421, 354–357.
Hong, Y.T., Jiang, H.B., Liu, T.S., Zhou, L.P., Beer, J., Li, H.D., Leng, X.T., Hong, B., Qin, X.G., 2000. Response of climate to solar forcing recorded in a 6000-year $\delta^{18}O$ time-series of Chinese peat cellulose. The Holocene 10, 1–7.
Hong, Y.T., Wang, Z.G., Jiang, H.B., Lin, Q.H., Hong, B., Zhu, Y.X., Wang, Y., Xu, L.S., Leng, X.T., Li, H.D., 2001. A 6000-year record of changes in drought and precipitation in northeastern China based on a $\delta^{13}C$ time series from peat cellulose. Earth Planet. Sci. Lett. 185, 111–119.
Hong, Y.T., Hong, B., Lin, Q.H., Zhu, Y.X., Shibata, Y., Hirota, M., Uchida, M., Leng, X.T., Jiang, H.B., Xu, H., Wang, H., Yi, L., 2003. Correlation between Indian Ocean summer monsoon and North Atlantic climate during the Holocene. Earth Planet. Sci. Lett. 211, 371–380.
Hong, Y.T., Hong, B., Lin, Q.H., Shibata, Y., Zhu, Y.X., Leng, X.T., Wang, Y., 2009. Synchronous climate anomalies in the western North Pacific and North Atlantic regions during the last 14,000 years. Quat. Sci. Rev. 28, 840–849.
Hong, B., Hong, Y.T., Lin, Q.H., Shibata, Y., Uchida, M., Zhu, Y.X., Leng, X.T., Wang, Y., Cai, C.C., 2010. Anti-phase oscillation of Asian monsoons during the Younger Dryas

period: evidence from peat cellulose $\delta^{13}C$ of Hani, Northeast China. Palaeogeogr. Palaeoclimatol. Palaeoecol. 297, 214–222.
Hong, B., Gasse, F., Uchida, M., Hong, Y.T., Leng, X.T., Shibata, Y., An, N., Zhu, Y.X., Wang, Y., 2014a. Increasing summer rainfall in arid eastern-Central Asia over the past 8500 years. Sci. Rep. 4, 5279. http://dx.doi.org/10.1038/srep05279.
Hong, B., Hong, Y.T., Uchida, M., Leng, X.T., Shibata, Y., Cai, C., Peng, H.J., Zhu, Y.X., Wang, Y., Yuan, L.G., 2014b. Abrupt variations of Indian and East Asian summer monsoons during the last deglacial stadial and interstadial. Quat. Sci. Rev. 97, 58–70.
Huang, R.H., Huang, G., 1999. Advances and problems needed for further investigation in the studies of the East Asian Summer Monsoon. Chin. J. Atmos. Sci. 23, 129–141 (in Chinese with English summary).
Ivanochko, T.S., Ganeshram, R.S., Brummer, G.J.A., Ganssen, G., Jung, S.J.A., Moreton, S.G., Kroon, D., 2005. Variations in tropical convection as an amplifier of global climate change at the millennial scale. Earth Planet. Sci. Lett. 235, 302–314.
Johnsen, S.J., Clausen, H.B., Dansgaard, W., Fuhrer, K., Gundestrup, N., Hammer, C.U., Iversen, P., Jouzel, J., Stauffer, B., Steffensen, J.P., 1992. Irregular glacial interstadials recorded in a new Greenland ice core. Nature 359, 311–313.
Kalnay, E., Kanamitsu, M., Kistler, R., Collins, W., Deaven, D., Gandin, L., Iredell, M., Saha, S., White, G., Woollen, J., Zhu, Y., Chellian, M., Ebisuzaki, W., Higgins, W., Janowiak, J., Mo, K.C., Ropelewski, C., Wang, J., Leetmaa, A., Reynolds, R., Jenne, R., Joseph, D., 1996. The NCER/NCAR 40-year reanalysis project. Bull. Am. Meteorol. Soc. 77, 437–471.
Knutti, R., Fluckiger, J., Stocker, T.F., Timmermann, A., 2004. Strong hemispheric coupling of glacial climate through freshwater discharge and ocean circulation. Nature 430, 851–856.
Koutavas, A., DeMenocal, P.B., Olive, G.C., Lynch-Stieglitz, J., 2006. Mid-Holocene El Niño–Southern Oscillation (ENSO) attenuation revealed by individual foraminifera in eastern tropical Pacific sediments. Geology 34, 993–996.
Kudrass, H.R., Hofmann, A., Doose, H., Emeis, K., Erlenkeuser, H., 2001. Modulation and amplification of climatic changes in the northern hemisphere by the Indian summer monsoon during the past 80 kyr. Geology 29, 63–66.
Kutzbach, J.E., 1981. Monsoon climate of the early Holocene: climate experiment with the earth's orbital parameters for 9000 years ago. Science 214, 59–61.
Kutzbach, J.E., Street-Perrott, F.A., 1985. Milankovitch forcing of fluctuations in the level of tropical lakes from 18 to 0 kyr BP. Nature 317, 130–134.
Landais, A., Masson-Delmotte, V., Stenni, B., Selmo, E., Roche, D.M., Jouzel, J., Lambert, F., Guillevic, M., Bazin, L., Arzel, O., Vinther, B., Gkinis, V., Popp, T., 2015. A review of the bipolar seeesaw from synchronized and high resolution ice core water stable isotope records from Greenland and East Antarctica. Quat. Sci. Rev. 114, 18–32.
Lee, X.Q., Feng, H.D., Guo, L.L., Wang, L.X., Jin, L.Y., Huang, Y.S., Chopping, M., Huang, D.K., Jiang, W., Jiang, Q., Cheng, H.G., 2005. Carbon isotope of bulk organic matter: a proxy for precipitation in the arid and semiarid central East Asia. Glob. Biogeochem. Cycles 19, GB4010. http://dx.doi.org/10.1029/2004GB002303.
Ménot, G., Burns, S.J., 2001. Carbon isotopes in ombrogenic peat bog plants as climatic indicators: calibration from an altitudinal transect in Switzerland. Org. Geochem. 32, 233–245.
Moy, C.M., Seltzer, G.O., Rodbell, D.T., Anderson, D.M., 2002. Variability of El Niño/Southern Oscillation activity at millennial timescales during the Holocene epoch. Nature 420, 162–165.
Müller, S.A., Joos, F., Edwards, N.R., Stocker, T.F., 2006. Water mass distribution and ventilation time scales in a cost-efficient, three-dimensional ocean model. J. Clim. 19, 5479–5499.
Nag, D., Phartiyal, B., 2015. Climatic variations and geomorphology of the Indus River valley, between Nimo and Batalik, Ladakh (NW Trans Himalayas) during Late Quaternary. Quat. Int. 371, 87–101.
Overpeck, J., Webb, R., 2000. Nonglacial rapid climate events: past and future. PNAS 97, 1335–1338.
Perry, C.A., Hsu, K.J., 2000. Geophysical, archaeological, and historical evidence support a solar-output model for climate change. Proc. Natl. Acad. Sci. 97, 12433–12438.
Reimer, P.J., Baillie, M.G.L., Bard, E., Bayliss, A., Beck, J.W., Blackwell, P.G., Ramsey, C.B., Buck, C.E., Burr, G.S., Edwards, R.L., Friedrich, M., Grootes, P.M., Guilderson, T.P., Hajdas, I., Heaton, T.J., Hogg, A.G., Hughen, K.A., Kaiser, K.F., Kromer, B., McCormac, F.G., Manning, S.W., Reimer, R.W., Richards, D.A., Southon, J.R., Talamo, S., Turney, C.S.M., van der Plicht, J., Weyhenmeyer, C.E., 2009. IntCal09 and Marine09 radiocarbon age calibration curves, 0–50,000 years cal BP. Radiocarbon 51, 1111–1150.
Ren, S.J., Yu, G.R., 2011. Carbon isotope composition ($\delta^{13}C$) of C3 plants and water use efficiency in China. Chin. J. Plant Ecol. 35, 119–124.
Rossignol-Strick, M., 1983. African monsoons, an immediate climate response to orbital insolation. Nature 304, 46–49.
Ruddiman, W.F., 2006. What is the timing of orbital-scale monsoon changes? Quat. Sci. Rev. 25, 657–658.
Schleser, G.H., 1995. Parameters determining carbon isotope ratios in plants. In: Frenzel, B., Stauffer, B., Weiss, M.M. (Eds.), Paläoklimaforschung, 15. Strasbourg, France, pp. 71–96.
Schulz, H., Von Rad, U., Erlenkeuser, H., 1998. Correlation between Arabian sea and Greenland climate oscillations of the past 110,000 years. Nature 393, 54–57.
Singh, D., Tsiang, M., Rajaratnam, B., Diffenbaugh, N.S., 2014. Observed changes in extreme wet and dry spells during the South Asian summer monsoon season. Nat. Clim. Chang. 4, 456–461.
Sirocko, F., Sarnthein, M., Erlenkeuser, H., Lange, H., Arnold, M., Duplessy, J.C., 1993. Century-scale events in monsoonal climate over the past 24,000 years. Nature 364, 322–324.
Sofer, Z., 1980. Preparation of carbon dioxide for stable carbon isotope analysis of petroleum fractions. Anal. Chem. 52, 1389–1391.
Staubwasser, M., Sirocko, F., Grootes, P.M., Segl, M., 2003. Climate change at the 4.2 kyr BP termination of the Indus valley civilization and Holocene south Asian monsoon variability. Geophys. Res. Lett. 30, 1425. http://dx.doi.org/10.1029/2002GL016822.
Stuiver, M., Grootes, P.M., 2000. GISP2 oxygen isotope rations. Quat. Res. 53, 277–283.
Teller, J.T., Leverington, D.W., Mann, J.D., 2002. Freshwater outbursts to the oceans from glacial Lake Agassiz and their role in climate change during the last deglaciation. Quat. Sci. Rev. 21, 879–887. http://dx.doi.org/10.1016/S0277-3791(01)00145-7.
Thamban, M., Purnachandra Rao, V., Schneider, R.R., Grootes, P.M., 2001. Glacial to Holocene fluctuations in hydrography and productivity along the southwestern continental margin of India. Palaeogeogr. Palaeoclimatol. Palaeoecol. 165, 113–127.
Thompson, L.G., Mosley-Thompson, E., Davis, M.E., Henderson, K.A., Brecher, H.H., Zagorodnov, V.S., Mashiotta, T.A., Lin, P.N., Mikhalenko, V.N., Hardy, D.R., Beer, J., 2002. Kilimanjaro ice core records: evidence of Holocene climate change in tropical Africa. Science 298, 589–593.
Tiwari, M., Ramesh, R., Bhushan, R., Sheshshayee, M.S., Somayajulu, B.K., Jull, A.J.T., Burr, G.S., 2010. Did the Indo-Asian summer monsoon decrease during the Holocene following insolation? J. Quat. Sci. 25, 1179–1188.
Turner, A.G., Annamalai, H., 2012. Climate change and the South Asian summer monsoon. Nat. Clim. Chang. 2, 587–595.
Uchida, M., Ohkushi, K., Kimoto, K., Inagaki, F., Inagaki, T., Tsunogai, U., TuZino, T., Shibata, Y., 2008. Radiocarbon-based carbon source quantification of anomalous isotopic foraminifera in last glacial sediments in the western North Pacific. Geochem. Geophys. Geosyst. 9, Q04N14. http://dx.doi.org/10.1029/2006GC001558.
van Geel, B., van der Plicht, J., Kilian, M.R., Klaver, E.R., Kouwenberg, J.H.M., Renssen, H., Reynaud-Farrera, I., Waterbolk, H.T., 1998. The sharp rise of $\Delta^{14}C$ ca. 800 cal BC: possible causes, related climatic teleconnections and the impact on human environments. Radiocarbon 40, 535–550.
Vonmoos, M., Beer, J., Muscheler, R., 2006. Large variations in Holocene solar activity - constraints from ^{10}Be in the GRIP ice core. J. Geophys. Res. 111, A10105. http://dx.doi.org/10.1029/2005JA011500.
Wang, Y., Cheng, H., Edwards, R.L., An, Z.S., Wu, J.Y., Shen, C.C., Dorale, J.A., 2001. A high-resolute absolute-dated Late Pleistocene monsoon record from Hulu Cave, China. Science 294, 2345–2348.
Wang, Y., Cheng, H., Edwards, R.L., He, Y., Kong, X., A., Z., Wu, J., Kelly, M.J., Dykoski, C.A., Li, X., 2005. The Holocene Asian monsoon: links to solar changes and North Atlantic climate. Science 308, 854–857.
Wang, G., Feng, X., Han, J., Zhou, L., Tan, W., Su, F., 2008. Paleovegetation reconstruction using $\delta^{13}C$ of soil organic matter. Biogeosciences 5, 1325–1337.
Wanner, H., Beer, J., Bütikofer, J., Crowley, T.J., Cubasch, U., Flückiger, J., Goosse, H., Grosjean, M., Joos, F., Kaplan, J.O., Küttel, M., Müller, S., Prentice, I.C., Solomina, O., Stocker, T.F., Tarasov, P., Wagner, M., Widmann, M., 2008. Mid- to late Holocene climate change: an overview. Quat. Sci. Rev. 27, 1791–1828.
Wanner, H., Solomina, O., Grosjean, M., Ritz, S.P., Jetel, M., 2011. Structure and origin of Holocene cold events. Quat. Sci. Rev. 30, 3109–3123.
Weiss, H., Raymond, S.B., 2001. What drives societal collapse? Science 291, 609–610.
Weiss, H., Courty, M.A., Wetterstrom, W., Guichard, F., Senior, R., Meadow, A., 1993. The genesis and collapse of third millennium North Mesopotamian civilization. Science 261, 995–1004.
Winkler, S., Matthews, J.A., 2010. Holocene glacier chronologies: are high-resolution global and interhemispheric comparisons possible? The Holocene 20, 1137–1147.
Wu, W.X., Liu, T.S., 2004. Possible role of the “Holocene Event 3” on the collapse of Neolithic cultures around the Central Plain of China. Quat. Int. 117, 153–166.
Yuan, D.X., Cheng, H., Edwards, R.L., Dykoski, C.A., Kelly, M.J., Zhang, M.L., Qing, J.M., Lin, Y.S., Wang, Y.J., Wu, J.Y., Dorale, J.A., An, Z.S., Cai, Y.J., 2004. Timing, duration, and transitions of the last interglacial Asian monsoon. Science 304, 575–578.